

# Effects of Oligomycin on Transient Currents Carried by $\text{Na}^+$ Translocation of *Bufo* $\text{Na}^+/\text{K}^+$ -ATPase Expressed in *Xenopus* Oocytes

Yanli Ding · Jingping Hao · Robert F. Rakowski

Received: 23 November 2010 / Accepted: 8 August 2011 / Published online: 30 August 2011  
© Springer Science+Business Media, LLC 2011

**Abstract**  $\text{Na}^+/\text{K}^+$ -ATPase (NKA) exports  $3\text{Na}^+$  and imports  $2\text{K}^+$  at the expense of the hydrolysis of 1ATP under physiological conditions. In the absence of  $\text{K}^+$ , it can mediate electroneutral  $\text{Na}^+/\text{Na}^+$  exchange. In the electroneutral  $\text{Na}^+/\text{Na}^+$  exchange mode, NKA produces a transient current containing fast, medium and slow components in response to a sudden voltage step. These three components of the transient current demonstrate the sequential release of  $\text{Na}^+$  ions from three binding sites. Our data from oocytes provide further experimental support for the existence of these components. Oligomycin is an NKA inhibitor that favors the  $2\text{Na}^+$ -occluded state without affecting the conformational state of the NKA. We studied the effects of oligomycin on both  $\text{K}^+$ -activated currents and transient currents in wild-type *Bufo* NKA and a mutant form of *Bufo* NKA, NKA: G813A. Oligomycin blocked almost all of the  $\text{K}^+$ -activated current, although the three components of the transient current showed different sensitivities to oligomycin. The oligomycin-inhibited charge movement measured using a P/4 protocol had a rate coefficient similar to the medium transient component. The fast component of the transient current elicited by a short voltage step also showed sensitivity to oligomycin. However, the slow component was not totally inhibited by oligomycin. Our results indicate that the second and third

sodium ions might be released to the extracellular medium by a mechanism that is not shared by the first sodium ion.

**Keywords**  $\text{Na}^+/\text{K}^+$ -ATPase · Oligomycin · Voltage clamp · *Xenopus laevis* oocyte · *Bufo marinus*

## Introduction

### The $\text{Na}^+/\text{K}^+$ ATPase Transport Cycle

$\text{Na}^+/\text{K}^+$ -ATPase (NKA) is an integral membrane protein that exports  $3\text{Na}^+$  and imports  $2\text{K}^+$  at the expense of the hydrolysis of 1ATP under physiological conditions. NKA pumps ions in a transport cycle usually referred to as the “Albers–Post scheme” (Albers 1967; Post et al. 1972; Skou and Esmann 1992). In this model, NKA can adopt two main conformations, E1 and E2, where ion-binding sites are facing the cytoplasm in E1 and the extracellular solution in E2. Phosphorylation of E1 by ATP promotes the occlusion (or trapping) of three intracellular  $\text{Na}^+$ , which are released to the external medium by a deocclusion transition associated with a conformational change to E2. Once two external  $\text{K}^+$  bind, they elicit dephosphorylation and  $\text{K}^+$  occlusion. ATP binding favors transition back to E1, prompting  $\text{K}^+$  release to the cytoplasm and binding of  $3\text{Na}^+$  to complete the cycle.

The voltage dependence of the outward pump current ( $I_p$ ) was determined by whole-cell patch clamp of isolated heart cells (Gadsby et al. 1985). An essentially voltage-insensitive transport cycle can be achieved by replacing external  $\text{Na}^+$  with large cations that are incompatible with transport, such as *N*-methyl D-glucamine (NMDG) (Rakowski and Paxson 1988; Gadsby et al. 1989; Rakowski et al. 1989; Sagar and Rakowski 1994), indicating that the major voltage-sensitive

Y. Ding · J. Hao · R. F. Rakowski  
Department of Biological Sciences, Ohio University,  
Athens, OH 45701, USA

Y. Ding (✉)  
Renal Division, Brigham and Women’s Hospital,  
Room 540, Harvard Institutes of Medicine, 4 Blackfan Circle,  
Boston, MA 02115, USA  
e-mail: yding5@partners.org

step is located in the  $\text{Na}_o^+$  deocclusion/occlusion and release/binding steps. This can be explained by postulating the existence of a narrow and deep access channel, or “ion well,” between the  $\text{Na}^+$  binding sites within the protein and the aqueous extracellular solution (Andersen et al. 1985; Lauser 1991; Gadsby et al. 1993).

$\text{Na}^+/\text{Na}^+$  exchange transport kinetics have been further examined through investigation of the transient currents elicited by sudden voltage steps. These currents are due to the influence of voltage on the rate constant of the system (Nakao and Gadsby 1986). Depolarizing and hyperpolarizing steps produced transient outward and inward currents, respectively, that decayed exponentially. The voltage dependence of the charge moved ( $Q$ ) was sigmoidal and saturated at large hyperpolarizing and depolarizing potentials. These data could be well fitted by a Boltzmann distribution

$$\frac{Q(V) - Q_{\min}}{Q_{\text{tot}}} = \frac{1}{1 + \exp\left[\frac{zF(V_{\text{mid}} - V)}{RT}\right]} \quad (1)$$

where  $Q_{\text{tot}}$  is the total amount of charge,  $Q_{\min}$  is the minimum value of charge reached at extreme negative voltages,  $V_{\text{mid}}$  is the midpoint voltage,  $z$  is apparent valence and  $R$ ,  $T$  and  $F$  have their usual meanings.  $RT/zF$  represents the steepness of the curve.

A fast component can be separated from a slow component of the transient current recorded from cardiac myocytes using giant patch clamp (Hilgemann 1994). The voltage dependence of the slow charge movement had a  $z$  value of 0.6, while the voltage dependence of the fast charge movement had a shallow slope with a  $z$  value of 0.26. A medium component of the transient currents was later detected, and the moveable charge in this component also exhibits a steep voltage dependence with a  $z$  value close to 1 (Holmgren et al. 2000). The three transient current components reflect the deocclusion/release of  $3\text{Na}^+$ , which occurs in sequence with decreasing time constants from the first (1 ms), to the second (about 0.3–0.05 ms) and finally the third ( $10^{-3}$  ms)  $\text{Na}^+$  ion (Holmgren et al. 2000). Studies on palytoxin-opened NKA showed that the second and third  $\text{Na}^+$  ions share the same pathway (Takeuchi et al. 2008). However, it is still not clear whether the first  $\text{Na}^+$  is released from its unique binding site to the extracellular medium through the same pathway, in spite of the availability of the crystal structures of NKA (Gadsby 2007; Morth et al. 2007).

#### The $\text{Na}^+/\text{K}^+$ -ATPase Inhibitor Oligomycin

Oligomycin is an inhibitor of ATP synthetase and NKA (Fahn et al. 1966). Oligomycin had no effect on the formation of the phosphorylated intermediate, even though it partially

inhibited  $\text{Na}^+$  efflux, in contrast with the inhibiting effect of ouabain on both the formation of the phosphorylated intermediate and  $\text{Na}^+$  efflux (Garrahan and Glynn 1967). Yoda and Yoda (1986) showed that there were three phosphorylated intermediate states in the absence of  $\text{K}^+$  and oligomycin. These were the  $\text{K}^+$ -sensitive E2P state, the ADP-sensitive E1P state and the  $\text{K}^+$ - and ADP-sensitive E\*P state. The specific state of the phosphorylated intermediate that was bound by oligomycin was defined by sensitivity of NKA to ADP and  $\text{K}^+$  in the presence of oligomycin. However, one potential drawback of this experimental design was that it might misrepresent E\*P as E1P (an ADP-sensitive,  $\text{K}^+$ -insensitive form) if oligomycin bound E\*P and blocked  $\text{K}^+$  from binding to NKA in this state. Therefore, E1P and possibly E\*P were suggested as the states that interacted with oligomycin (Yoda and Yoda 1986).

The  $3\text{Na}^+$  occluded form of NKA, E1P( $\text{Na}_3$ ), was proposed as the conformation favored by oligomycin (Glynn and Karlsh 1990). However, the number of  $\text{Na}^+$  bound to NKA in the presence of oligomycin has been shown to be dependent on the concentration of  $\text{Na}^+$  in the solution (Esmann and Skou 1985), and the effect of oligomycin depended on the binding of  $\text{Na}^+$  to its unique binding site. In addition, oligomycin did not affect the conformational change from E1 to E2 when  $\text{Na}^+$  was replaced by  $\text{Na}^+$  congeners (Esmann and Skou 1985). We therefore hypothesize that the conformation that oligomycin reacts with is adjacent to the  $\text{Na}^+$ -releasing step at its specific binding site to the extracellular medium. This could be either E1P( $\text{Na}_3$ ) or E2P- $2\text{Na}$ , assuming that the first  $\text{Na}^+$  released to the extracellular medium is from the specific binding site (Holmgren et al. 2000).

Oligomycin was utilized in transient current studies of endogenous *Xenopus* NKA, and it inhibited about 80% of the charge translocation carried by the electroneutral  $\text{Na}^+/\text{Na}^+$  exchange (Holmgren and Rakowski 1994). Here, we further investigated the effect of oligomycin on charge translocation, and our results directly demonstrate the existence of three transient current components. Of these three, the slow component could exist independently.

## Materials and Methods

### Oocyte Maintenance and Expression

*Xenopus laevis* oocytes at stages V–VI were collected and treated with 0.3% collagenase in  $\text{Ca}^{2+}$ -free ND96 solution (96 mM NaCl, 2 mM KCl, 1 mM  $\text{MgCl}_2$ , 2.5 mM Na pyruvate, 5 mM Tris HEPES, pH 7.3, osmolarity =  $200 \pm 5$ ) for 40–60 min to remove the follicular layer. Oocytes remained viable for up to 6 days at  $15^\circ\text{C}$  in ND96 solution ( $\text{Ca}^{2+}$ -free ND96 plus 1.8 mM  $\text{CaCl}_2$ ).

Wild-type *Bufo marinus* NKA  $\alpha_1$  and  $\beta_1$  cRNA were transcribed from their corresponding cDNAs. Site-directed mutations were introduced into *Bufo*  $\alpha_1$ -subunit using the QuikChange® II Site-Directed Mutagenesis Kit (Stratagene, La Jolla, CA). Wild-type and mutant  $\alpha_1$ -subunits were expressed by coinjection of 10 ng  $\alpha_1$  cRNA with 1 ng  $\beta_1$  cRNA into oocytes 1 day after oocytes were collected. Injected oocytes were incubated in ND96 solution for 3 days to obtain good membrane expression. Oocytes were incubated overnight in 0.2  $\mu$ M ouabain containing ND96 solution to inhibit the endogenous *X. laevis* NKA. *B. marinus*  $\alpha_1$  is more ouabain-resistant than *X. laevis*  $\alpha_1$ , so pretreatment in 0.2  $\mu$ M ouabain inhibits the endogenous NKA but not the introduced *Bufo* NKA (Jaisser et al. 1992), while the application of 1 mM ouabain during electrophysiological measurement inhibits *Bufo* NKA.

### Electrophysiological Measurements

$I_p$  mediated by *Bufo* NKA was studied using a two-electrode oocyte voltage-clamp preparation. Voltage pulses of 100 ms duration were applied every 300 ms from a holding potential ( $V_h$ ) of  $-20$  mV to command potentials over the range  $-120$  to  $+60$  mV in increments of 20 mV. Data were acquired using an analog to digital converter system and software (TL-1 DMA interface, 100 KHz, PCLAMP, version 9; Molecular Devices, Sunnyvale, CA) running on a standard personal computer system (Dell Computer, Austin, TX). The analog signal was sampled every 100  $\mu$ s (10 KHz).

We calculated the oligomycin-sensitive currents ( $I_{\text{oligo}}$ ) and the ouabain-sensitive current ( $I_{\text{ouab}}$ ) at a holding potential of  $-20$  mV. The currents in the presence of 5 mM  $K^+$  were subtracted by the currents obtained after the addition of oligomycin in different concentrations or with the addition of 1 mM ouabain, respectively, using ClampFit (v9.2; Automate Scientific, Berkeley, CA) software.  $I_{\text{ouab}}$  is treated as total available  $I_p$  because ouabain is assumed to completely block pump current. The dependence of  $I_p$  on oligomycin was further analyzed with a least-squares fitting procedure using SIGMAPLOT (v8.0; Systat Software, Richmond, CA) in order to determine the fit parameters. All experiments were performed at room temperature ( $\sim 22^\circ\text{C}$ ).

Transient currents were measured using an oocyte cut-open voltage-clamp setup, as described recently (Ding and Rakowski 2010). Three protocols were utilized in order to examine the inhibition of the transient current by oligomycin. (1) A 12 long  $I$ - $V$  step protocol was used to determine the voltage dependence of charge movement. Voltage pulses of 40 ms in duration were applied every 300 ms from  $V_h$  of  $-20$  mV to command potentials over the range  $-160$  to  $+60$  mV in increments of 20 mV. The final current records were obtained by averaging four repetitions of the pulse protocol. The analog signal was low

pass-filtered at 5 KHz before being digitized and sampled every 20  $\mu$ s. (2) A 2 short  $I$ - $V$  step protocol was used to resolve the very fast component. Two 20 ms voltage steps ( $+40$  and  $-160$  mV) were made from a  $V_h$  of  $-20$  mV. The analog signal was low pass-filtered at 10 KHz before being digitized and sampled every 10  $\mu$ s. The transient current measured using either (1) or (2) was calculated by subtracting the current records obtained after arresting  $\text{Na}^+/\text{Na}^+$  exchange by the addition of 1 mM ouabain or oligomycin in different concentrations from the currents acquired just prior to the addition of the inhibitor. (3) A P/4 protocol was used to avoid contamination due to linear capacitance (Bezanilla and Armstrong 1977). Voltage pulses of 40 ms in duration were made from  $V_h$   $-20$  mV to command potentials over the range  $-160$  to  $+60$  mV in increments of 20 mV. Four small voltage steps with one-quarter magnitude from a holding potential of  $-180$  mV were applied before a voltage step from  $V_h$   $-20$  mV was applied in the same direction. The subsequent subtraction of currents elicited by these small voltage steps from the current measured by the following voltage step resulted in elimination of the linear capacitive current.

To obtain the relaxation rate, the transient current was fitted with either a single exponential or a two-component exponential function. The charge translocated was determined by direct numerical integration of the transient currents or by multiplying the initial value ( $A$ ) and time constant ( $\tau$ ) obtained by the exponential fit using Clampfit 9.2 software. Further analysis, least-squares curve fitting and preparation of figures were done with SIGMAPLOT 8.0. Curve fit parameters were obtained from the least-squares fitting procedure. Experiments were performed at room temperature ( $\sim 22^\circ\text{C}$ ).

### Solutions

Two  $K^+$ -free solutions, 100 $\text{Na}^+$  external solution and 10 $\text{Na}^+$  internal solution, were used for the cut-open oocyte preparation. The 100 $\text{Na}^+$  external solution had the following composition: 100 mM Na glutamate, 20 mM tetraethylammonium (TEA) glutamate, 3 mM Mg glutamate, 5 mM  $\text{Ba}(\text{NO}_3)_2$ , 2 mM  $\text{Ni}(\text{NO}_3)_2$ , 0.01 mM  $\text{Gd}(\text{NO}_3)_3$ , 0.3 mM niflumic acid and 10 mM Tris HEPES (pH 7.6). The composition of the 10 $\text{Na}$  internal solution was 10 mM Na glutamate, 20 mM TEA glutamate, 10 mM  $\text{MgSO}_4$ , 5 mM MgATP, 5 mM TrisADP, 5 mM 1,2-bis(2-amino-phenoxy)ethane- $N,N,N',N'$ -tetraacetic acid (BAPTA), 70 mM NMDG glutamate, 10 mM MOPS (pH 7.3). Note that both ATP and ADP were present in the internal solution to promote electroneutral  $\text{Na}^+/\text{Na}^+$  exchange (De Weer 1970; Glynn and Hoffman 1971). One millimolar AP5A was included to prevent phosphate exchange between ATP and ADP. The solutions were designed to

minimize any non-pump-mediated current. Extracellular TEA<sup>+</sup> and Ba<sup>2+</sup> were present to block passive K<sup>+</sup> conductance (Holmgren and Rakowski 1994). NMDG was used as an internal Na<sup>+</sup> substitute because it would be less likely to compete for Na<sup>+</sup> binding sites than smaller cations. The solutions were nominally chloride-free and are also Ca<sup>2+</sup>-free to prevent activation of any Ca<sup>2+</sup>-dependent anionic current. Niflumic acid was used to block the Cl<sup>-</sup> channel, while Ni<sup>2+</sup> and Gd<sup>3+</sup> were added to block Na<sup>+</sup>/Ca<sup>2+</sup> exchange (Kimura et al. 1987) and stretch-activated cation channels (Yang and Sachs 1989), respectively. Two forms of oligomycin were used in our NKA studies. One was an oligomycin mixture (Sigma, St. Louis, MO) consisting of 65% oligomycin A and oligomycin B and C in undetermined percentages according to the manufacturer, and the other was pure oligomycin B (US Biological, Swampscott, MA); both were dissolved in DMSO. The concentration of DMSO in all of the final solutions was kept constant throughout experiments on a single oocyte, and DMSO has no effect on the  $I_p$  mediated by NKA (Rakowski et al. 1989). For the oocyte voltage-clamp preparation, the perfusing solutions had the same composition as the 100Na external solution with the addition of either 5 mM TMA or 5 mM K<sup>+</sup>.

## Results

### Inhibition by Oligomycin of $I_p$ Mediated by Wild-Type *Bufo* NKA

Oocytes were initially perfused with 0 K<sup>+</sup> solution, then changed to solutions containing 5 mM K<sup>+</sup>. The inhibition of K<sup>+</sup>-activated  $I_p$  by the oligomycin mix was investigated by gradually increasing the concentration of oligomycin. Finally, in the presence of a saturating concentration of oligomycin, 1 mM ouabain was added to eliminate any remaining  $I_p$ . The  $I$ - $V$  relationships are shown in Fig. 1a. The applied voltage range was not large enough to determine the voltage dependence of the  $I_p$  mediated by wild-type *Bufo* NKA, so we were not able to characterize the  $I$ - $V$  relationships in the absence and presence of oligomycin. There was little residual current at an oligomycin concentration of 120  $\mu$ g/ml. The ratio  $I_{\text{oligo}}/I_{\text{ouab}}$  at a membrane potential of 0 mV was plotted against oligomycin concentration ( $[\text{oligo}]$ ) to show the dose dependence curve for the inhibition of  $I_p$  by oligomycin (Fig. 1b). The apparent affinity of NKA for oligomycin was obtained through fitting to Eq. 2

$$I_{\text{oligo}}/I_{\text{ouab}} = a * [\text{Oligo}]/(K_i + [\text{Oligo}]) \quad (2)$$

where  $a$  is the maximum inhibition by oligomycin and  $K_i$  is the apparent affinity for oligomycin. In this set of studies,

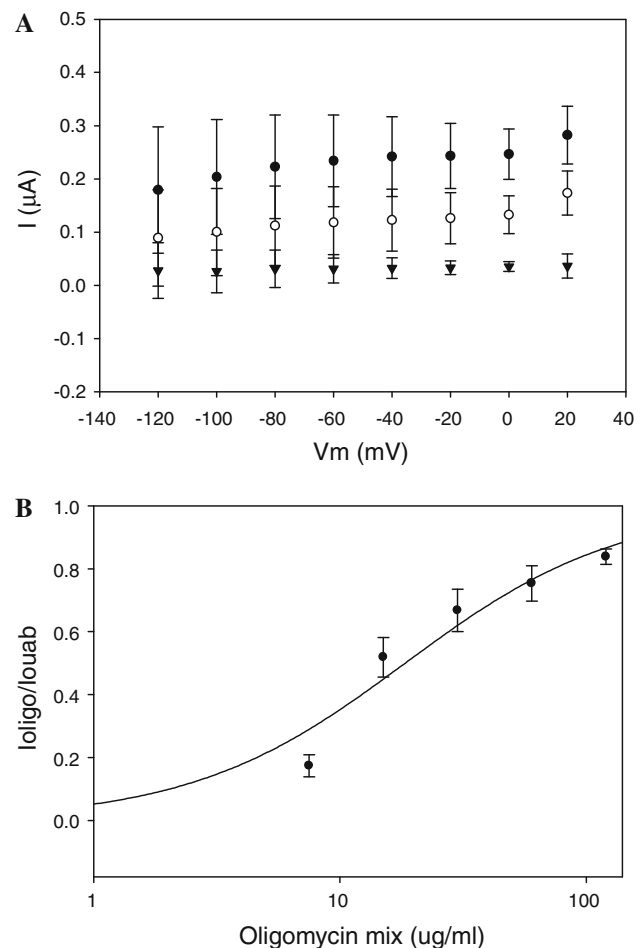


**Fig. 1** The inhibiting effect of oligomycin on 5 mM K<sup>+</sup>-activated current mediated by wild-type *Bufo* NKA. **a**  $I$ - $V$  relationship before (filled circles) and after the addition of 15  $\mu$ g/ml (empty circles) and 120  $\mu$ g/ml oligomycin (filled triangles). **b** Dose-response curve of K<sup>+</sup>-activated current versus oligomycin concentration. Solid line represents best fit to Eq. 2, with best fit parameters:  $K_i = 18.4 \pm 4.5$   $\mu$ g/ml and  $a = 99.9\%$

the apparent affinity for the oligomycin mix was  $18.4 \pm 4.5$   $\mu$ g/ml and the maximum inhibition was 99.9%.

### Inhibition by Oligomycin of $Q_{\text{all}}$ of Transient Currents

The apparent affinity for oligomycin was also obtained by determining its inhibiting effect on charge movement during the whole “on” traces (the whole trace was integrated to get  $Q_{\text{all}}$ ). Pump-mediated charge movement was measured first in the absence of oligomycin and ouabain, then in the presence of oligomycin at increasing concentrations and then in the presence of 1 mM ouabain. Transient currents in the presence of ouabain were subtracted from transient currents under all other conditions to get the pump-specific currents. Representative subtracted transient currents elicited by a voltage step from  $-20$  to  $-160$  mV

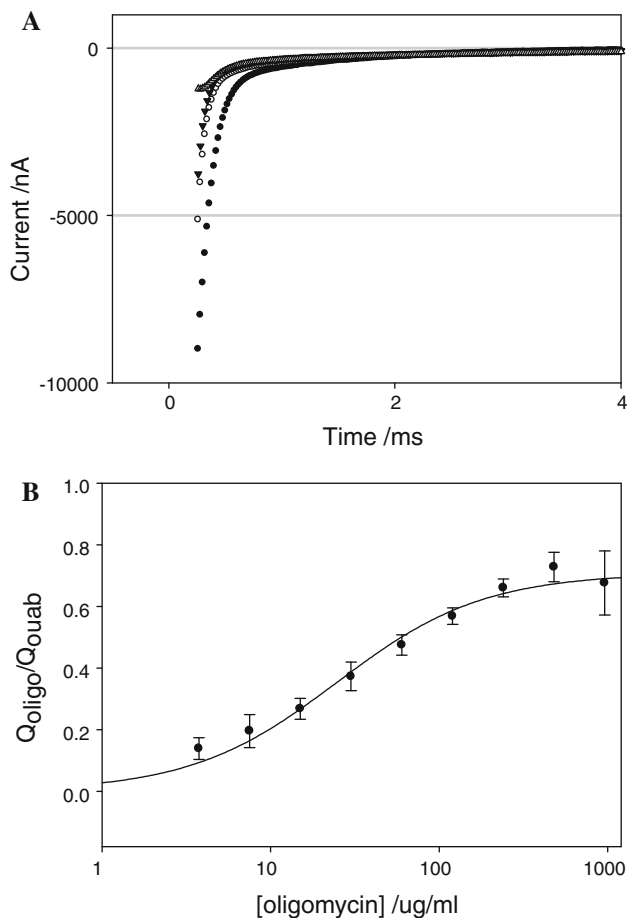


**Fig. 2** The inhibiting effect of oligomycin on transient currents mediated by wild-type *Bufo* NKA. **a** Representative transient currents elicited by a voltage step of  $-160$  mV in the absence of oligomycin (filled circles) and in the presence of  $15$   $\mu\text{g/ml}$  (empty circles),  $30$   $\mu\text{g/ml}$  (filled triangles) and  $960$   $\mu\text{g/ml}$  (empty triangles) oligomycin. **b** Dose-response curves of oligomycin inhibition of *Bufo* NKA. Data points (mean  $\pm$  SE) represent  $Q_{\text{all}}$  inhibited by a certain oligomycin concentration. Solid line represents the best fit to Eq. 3, with best fit parameters:  $K_i = 24.8 \pm 4.1$   $\mu\text{g/ml}$  and  $b = 70.8 \pm 3.0\%$

at  $0$ ,  $15$ ,  $30$  and  $960$   $\mu\text{g/ml}$  oligomycin are shown in Fig. 2a. The amount of charge inhibited by oligomycin at different concentrations ( $Q_{\text{oligo}}$ ) relative to the total charge moved by NKA ( $Q_{\text{ouab}}$ ),  $Q_{\text{oligo}}/Q_{\text{ouab}}$ , was plotted to show the apparent affinity for oligomycin and its maximum inhibiting effect (Fig. 2b). The data were fitted by Eq. 3,

$$Q_{\text{oligo}}/Q_{\text{ouab}} = b * [\text{oligo}] / (K_i + [\text{oligo}]) \quad (3)$$

where  $b$  is the maximum inhibition by oligomycin and  $K_i$  is the apparent affinity for oligomycin. In these experiments,  $K_i$  was calculated to be  $24.8 \pm 4.1$   $\mu\text{g/ml}$  and the maximum inhibition as  $70.8\%$ . A  $t$ -test did not reveal a statistically significant difference between  $K_i$  determined in these conditions and that ( $18.4 \pm 4.5$   $\mu\text{g/ml}$ ) calculated in the presence of potassium ( $P = 0.334$ ).

### Dominant Inhibition by Oligomycin of Faster Current Components

Figure 3 shows the average current records from seven oocytes. Oligomycin ( $120$   $\mu\text{g/ml}$ ) was added to determine the oligomycin-sensitive current before the addition of  $1$  mM ouabain to inhibit the residual current insensitive to  $120$   $\mu\text{g/ml}$  oligomycin. For the oligomycin-sensitive current, the peak transient currents at  $-160$  mV and at  $+60$  mV were  $-2,000$  and  $+1,500$  nA, respectively, and occurred within  $0.4$  ms after voltage change. The peak of oligomycin-insensitive transient currents had a much smaller magnitude ( $-1,000$  nA at  $-160$  mV and  $800$  nA at  $60$  mV) and a  $0.1$ -ms delay compared to the oligomycin-sensitive transient currents (Fig. 3). Small time-dependent leak currents from the same oocytes are shown in Fig. 3D.

$Q_{\text{all}}$  was calculated from the oligomycin-insensitive currents in these oocytes and from ouabain-sensitive transient currents in another set of oocytes that were not treated with oligomycin. The application of oligomycin decreased the steepness of  $Q_{\text{all}}$ , which was reflected as an increase of  $z$  from  $0.4$  to  $0.56$  (Fig. 4). In addition, the application of oligomycin shifted the  $Q_{\text{all}}$  vs.  $V$  curve to the right, which increased  $V_{\text{mid}}$  from  $-67$  to  $-51$  mV.

### Effect of Oligomycin on Transient Current Mediated by Mutant *Bufo* NKA: G813A

Figure 3B, C shows subtracted currents, which are generally contaminated with time-dependent leak currents, like the ones shown in Fig. 3D. Therefore, a P/4 protocol was employed to eliminate the leak currents. Compared to the subtracted ouabain/oligomycin-sensitive current, the non-linear capacitance determined from the P/4 protocol has no time-dependent leak current, and changes in linear capacitance over time are therefore eliminated. However, the P/4 protocol cannot be used on wild-type *Bufo* NKA because its  $Q_v$  does not reach a plateau at the oocyte-tolerable voltage range (Figs. 4, 5). G813A is a mutant form of *Bufo* NKA  $\alpha_1$ -subunit (Li et al. 2005), where the replacement of glycine by alanine increased both intracellular and extracellular  $\text{Na}^+$  apparent affinity but did not modify the kinetics of a conformational change (Li et al. 2005). Due to its effect of promoting  $\text{Na}^+$  binding, thus favoring E1, the  $Q$ - $V$  curve is significantly shifted to the right, which makes it possible to employ the P/4 protocol to determine the nonlinear capacitance mediated by NKA (Fig. 5).

A saturating concentration of oligomycin ( $120$   $\mu\text{g/ml}$ ) was applied in order to determine its effect on transient currents. Two voltage jumps,  $-160$  and  $+20$  mV, were used as representatives; and at each voltage, two transient currents were analyzed, the transient inhibited by oligomycin and the transient that was not sensitive to



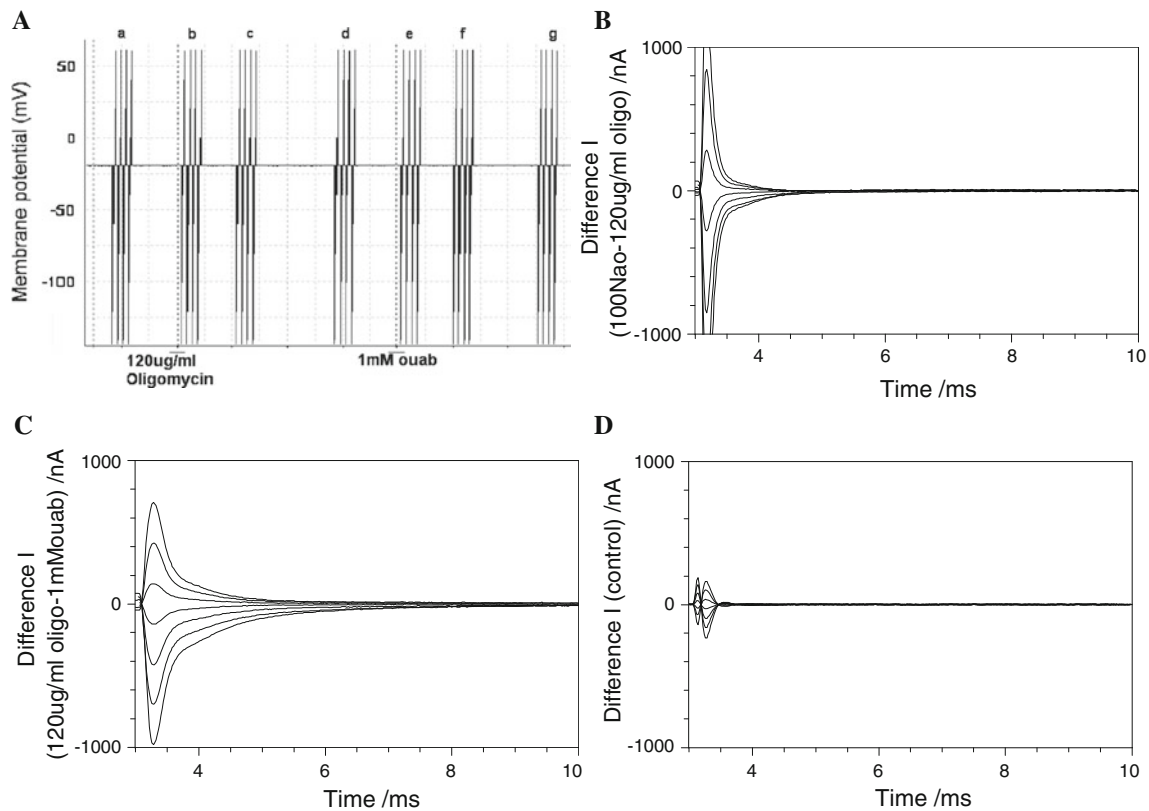


**Fig. 3** The average 120  $\mu\text{g/ml}$  oligomycin-sensitive and -insensitive transient currents measured in oocytes internally incubated with 10 mM  $\text{Na}^+$  0  $\text{K}^+$  and externally perfused with 100 mM  $\text{Na}^+$  0  $\text{K}^+$  solutions. **A** The chart view of an entire experiment with voltage steps labeled as *a*–*g* applied under different conditions. Difference currents elicited by voltage steps to  $-160$ ,  $-120$ ,  $-80$ ,  $-40$ ,  $0$ ,  $40$  and  $60$  mV

under different conditions are shown in **B–D**. **B** Transient currents inhibited by 120  $\mu\text{g/ml}$  oligomycin (*a*–*c*). **C** Transient currents that were oligomycin-insensitive but inhibited by 1 mM ouabain (*d*–*f*). **D** Control obtained by subtracting ouabain-inhibited current transients (*e*–*g*) that had similar durations compared to *a*–*c* and *d*–*f*. Data are from seven oocytes

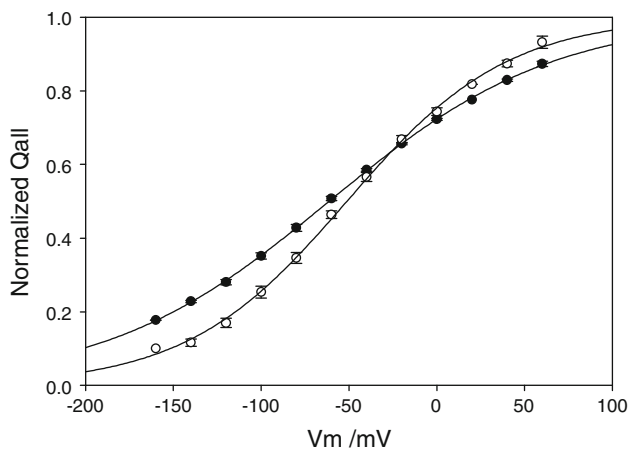


**Fig. 4** Comparison of ouabain-sensitive  $Q_{\text{all}}$  in the presence and absence of 120  $\mu\text{g/ml}$  oligomycin. Symbols represent data points (mean  $\pm$  SE) in the absence (filled circles) or presence (empty circles) of oligomycin, and the solid lines represent the best fit using Eq. 1, with best fit parameters:  $V_{\text{mid}} = -67.0 \pm 3.5$  mV and  $z = 0.40 \pm 0.02$  in the absence of oligomycin,  $V_{\text{mid}} = -51.2 \pm 2.5$  mV and  $z = 0.56 \pm 0.04$  in the presence of oligomycin. Both sets of data were obtained from seven oocytes

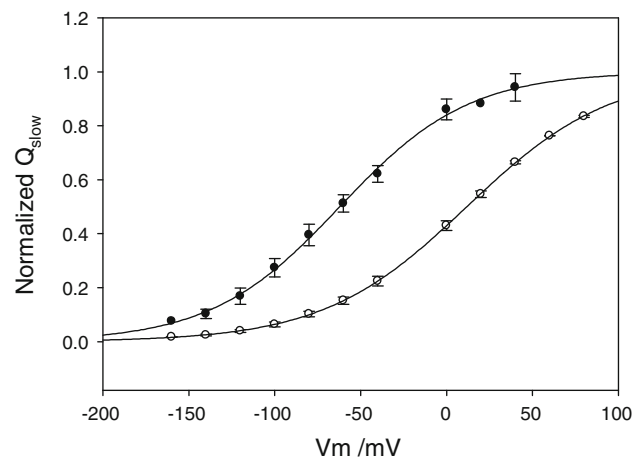


**Fig. 5** Voltage dependence of  $Q_{\text{slow}}$  mediated by wild-type *Bufo* NKA (filled circles) and *Bufo* NKA: G813A (empty circles). Symbols represent data points (mean  $\pm$  SE), and solid lines represent the best fits by Eq. 1, with best fit parameters:  $V_{\text{mid}} = -62.2 \pm 4.8$  mV and  $z = 0.68 \pm 0.11$  for *Bufo* wild-type NKA,  $V_{\text{mid}} = 11.8 \pm 3.1$  mV and  $z = 0.61 \pm 0.03$  for *Bufo* NKA: G813A. Each data set was obtained from five oocytes from at least two frogs

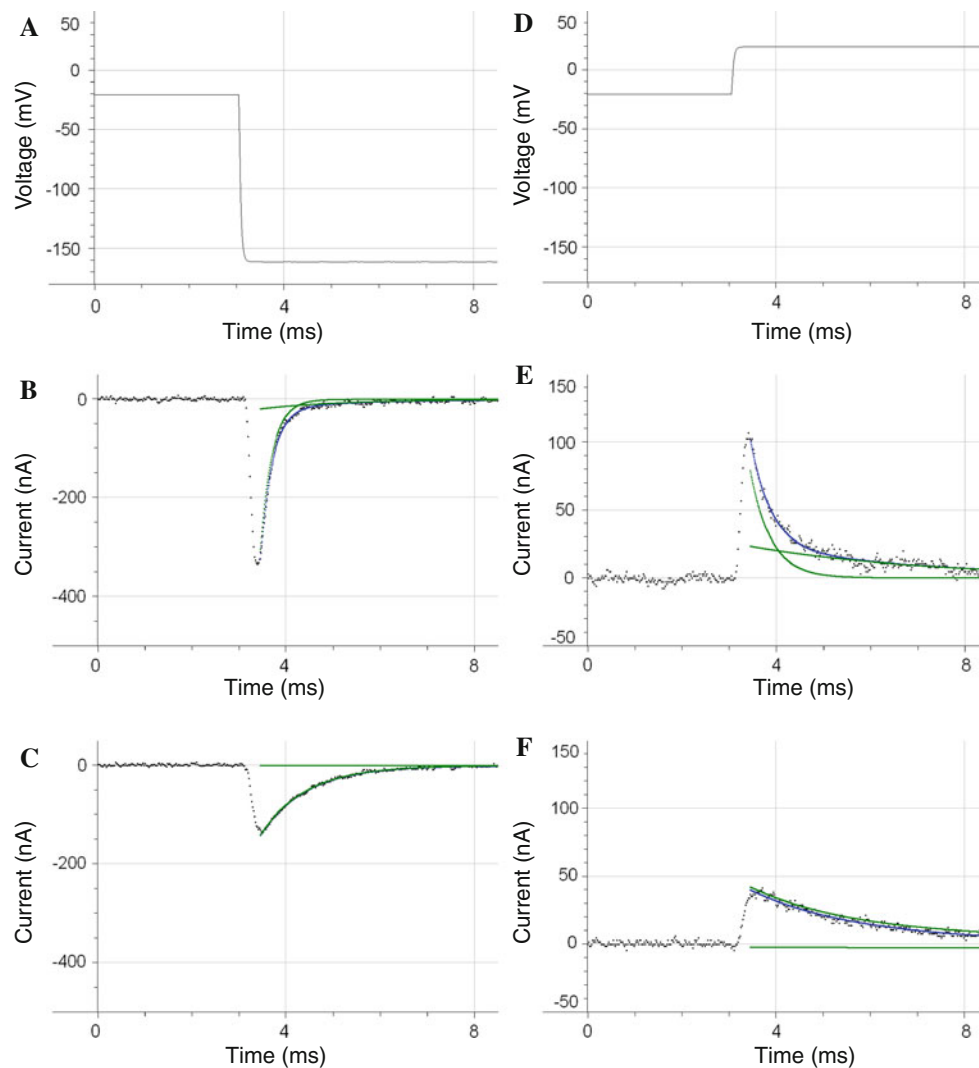


**Fig. 6** The inhibition by 120  $\mu\text{g/ml}$  oligomycin of transient current mediated by *Bufo* NKA: G813A. The experiment was performed in 100 mM  $\text{Na}^+$  0 K external solution. Transient currents (**b**, **c**, **e** and **f**) were elicited by voltage steps from  $-20$  to  $-160$  mV (**a**) and from  $-20$  to  $20$  mV (**d**). **b** and **c** were elicited by the step shown in **a**, and **e** and **f** were elicited by the step shown in **d**. Linear capacitive current was subtracted using the P/4 protocol. Blue line represents the best fit using a two-exponential function. The two green lines represent the two fitted components. **b** Oligomycin-sensitive transient current at  $-160$  mV, with best fit parameters:  $A_1 = -20 \pm 2$  nA,  $\tau_1 = 1.74 \pm$

$0.19$  ms,  $A_2 = -305 \pm 3$  nA,  $\tau_2 = 0.26 \pm 0.004$  ms. **c** Oligomycin-insensitive transient at  $-160$  mV, with best fit parameters:  $A_1 = -0.04 \pm 0.08$  nA,  $\tau_1 = -4.7 \pm 2.5$  ms,  $A_2 = -141 \pm 0.6$  nA,  $\tau_2 = 0.97 \pm 0.01$  ms. **e** Oligomycin-sensitive transient current at  $20$  mV, with best fit parameters:  $A_1 = 23 \pm 1$  nA,  $\tau_1 = 3.8 \pm 0.3$  ms,  $A_2 = -79 \pm 2$  nA,  $\tau_2 = 0.44 \pm 0.02$  ms. **f** Oligomycin-insensitive transient at  $20$  mV, with best fit parameters:  $A_1 = -3 \pm 13$  nA,  $\tau_1 = -73 \pm 120$  ms,  $A_2 = -37 \pm 0.5$  nA,  $\tau_2 = 3.3 \pm 0.1$  ms

oligomycin. For all transient currents, we utilized a two-exponential function to fit the data in order to distinguish faster from slower components in the total transient current. The fit to the 120  $\mu\text{g/ml}$  oligomycin-sensitive transient current revealed a small slower component, with  $A_1 = -20$  nA and  $\tau_1 = 1.74$  ms, and a dominant faster component, with  $A_2 = -305$  nA and  $\tau_2 = 0.26$  ms (Fig. 6b). The fit to the oligomycin-insensitive current had only one dominant slow component, with  $A = -141$  nA

and  $\tau \approx 1$  ms (Fig. 6c). The magnitude of the other component,  $A_1 = -0.04 \pm 0.08$  nA, was close to zero. The addition of 120  $\mu\text{g/ml}$  oligomycin therefore sufficiently separated two components of the transient current at  $-160$  mV.

The transient current elicited by the voltage jump to  $+20$  mV was also analyzed for its sensitivity to oligomycin (Fig. 6d-f). The fit to the oligomycin-sensitive transient current also consisted of two components, a slower one,

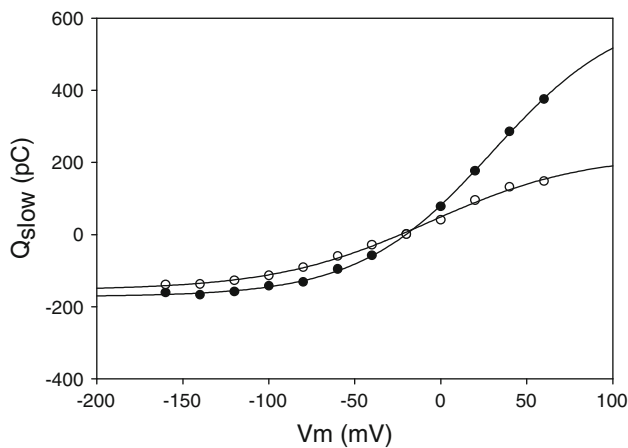


**Fig. 7** Voltage dependence of  $Q_{\text{slow}}$  before and after the addition of 120  $\mu\text{g/ml}$  oligomycin. Symbols represent data points before (filled circles) or after (empty circles) adding oligomycin, and solid lines represent the best fits by Eq. 1, with best fit parameters:  $Q_{\text{tot}} = 800 \pm 37$  pC,  $V_{\text{mid}} = 30 \pm 3.6$  mV and  $z = 0.66 \pm 0.03$  before adding oligomycin;  $Q_{\text{tot}} = 377 \pm 32$  pC,  $V_{\text{mid}} = -7 \pm 6.3$  mV and  $z = 0.56 \pm 0.06$  after adding oligomycin. Data are from the same oocyte expressing mutant *Bufo* NKA: G813A as in Figs. 5 and 6

with  $A_1 = 23$  nA and  $\tau_1 = 3.79$  ms, and a faster one, with  $A_2 = 79$  nA and  $\tau_2 = 0.44$  ms (Fig. 6e). The fit to the oligomycin-insensitive current contained only one dominant component with  $\tau \approx 2.3$  ms and  $A = 37$  nA (Fig. 6f). Therefore, the addition of 120  $\mu\text{g/ml}$  oligomycin inhibited the faster component completely and the slower component partially at 20 mV.

The voltage dependence of  $Q_{\text{slow}}$  before and after the addition of oligomycin is plotted in Fig. 7. The addition of oligomycin decreased  $Q_{\text{slow}}$  by about 50%, and the decrease occurred mainly at positive membrane potentials.  $V_{\text{mid}}$  of  $Q_{\text{slow}}$  after the addition of oligomycin shifted from 30 to  $-7$  mV (Fig. 7), which was opposite to the inhibiting effect by oligomycin of total charge movement mediated by wild-type *Bufo* NKA (Fig. 4).

The fast component with a shallow  $Q$ - $V$  curve (Hilgemann 1994; Holmgren et al. 2000) cannot be observed using the P/4 protocol. Additional experiments were therefore required to demonstrate the inhibiting effect of oligomycin on this component. In order to minimize the amount of DMSO and the lipophilic oligomycin mixture, pure oligomycin B was utilized. Oligomycin B was referred to as the effective component at inhibiting the NKA in some studies (Nakao and Gadsby 1986; Holmgren and Rakowski 1994). The  $I_p$  mediated by *Bufo* NKA: G813A was measured as a function of oligomycin, and Fig. 8 shows representative  $I$ - $V$  relationships in the presence of 0, 3.2 and 12.8  $\mu\text{M}$  oligomycin B. The  $I$ - $V$  curve of G813A had a sigmoid shape ( $z = 1$ ) at the applied voltage range, which is in contrast to the lack of voltage dependence of  $I_p$

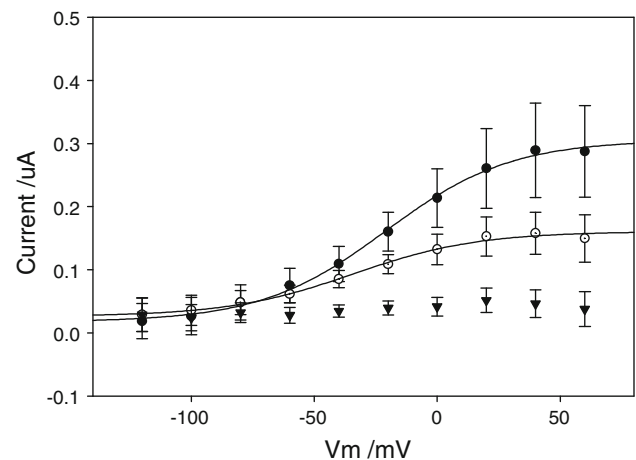


**Fig. 8** The inhibiting effect of oligomycin B on 5 mM  $\text{K}^+$ -activated current mediated by mutant *Bufo* NKA: G813A. The experiment was done in  $100\text{Na}^+$  solution. Symbols represent data points (filled circle 0  $\mu\text{M}$  oligo B, empty circles 3.2  $\mu\text{M}$  oligo B and triangles 12.8  $\mu\text{M}$  oligo B). Solid lines are the best fit curves using the Boltzmann equation with a slope of 1. Data were from three oocytes from at least two frogs

of wild-type *Bufo* NKA (Fig. 1). This difference at our applied voltage range is accounted for by the fact that a higher apparent binding affinity to  $\text{Na}^+$  caused a rightward shift of the  $I$ - $V$  curves in *Bufo* NKA: G813A. Oligomycin B at 3.2  $\mu\text{M}$  inhibited about half of the  $I_p$  activated by 5 mM  $\text{K}^+$ , but it did not change the steepness of the  $I$ - $V$  relationship (Fig. 8). NKA still carried one net charge per cycle out of the cell at an oligomycin B concentration of 3.2  $\mu\text{M}$ . Oligomycin at 12.8  $\mu\text{M}$  achieved nearly maximal inhibition of  $I_p$ , and the  $K_i$  of *Bufo* NKA: G813A for oligomycin B was determined to be 3.9  $\mu\text{M}$  (3  $\mu\text{g/ml}$ ) in our study (data not shown), which is close to the previously published 1.4  $\mu\text{M}$  (Arato-Oshima et al. 1996). If 20% of the oligomycin mixture is oligomycin B (Yoda and Yoda 1986), this is equivalent to about 15  $\mu\text{g/ml}$  of the oligomycin mixture.

The subtracted ouabain-sensitive or oligomycin-sensitive transients were used to resolve the fast current with a shallow slope. To minimize contamination due to linear capacitance, protocol (2) was applied to minimize the stress on oocytes. Our experiments were intended to show whether oligomycin can affect the existence of the fast component. The fast component had a rate of  $10^6/\text{S}$ , previously published by Holmgren and colleagues (2000); and as our sampling rate was limited to 100 kHz, the exact kinetics of the fast component could not be determined. Two different concentrations of oligomycin B were utilized in this method to show the direct inhibiting effect of oligomycin B on the fast component. Oligomycin B (3.2  $\mu\text{M}$ ) inhibited only a part of the fast component with  $\tau$  close to



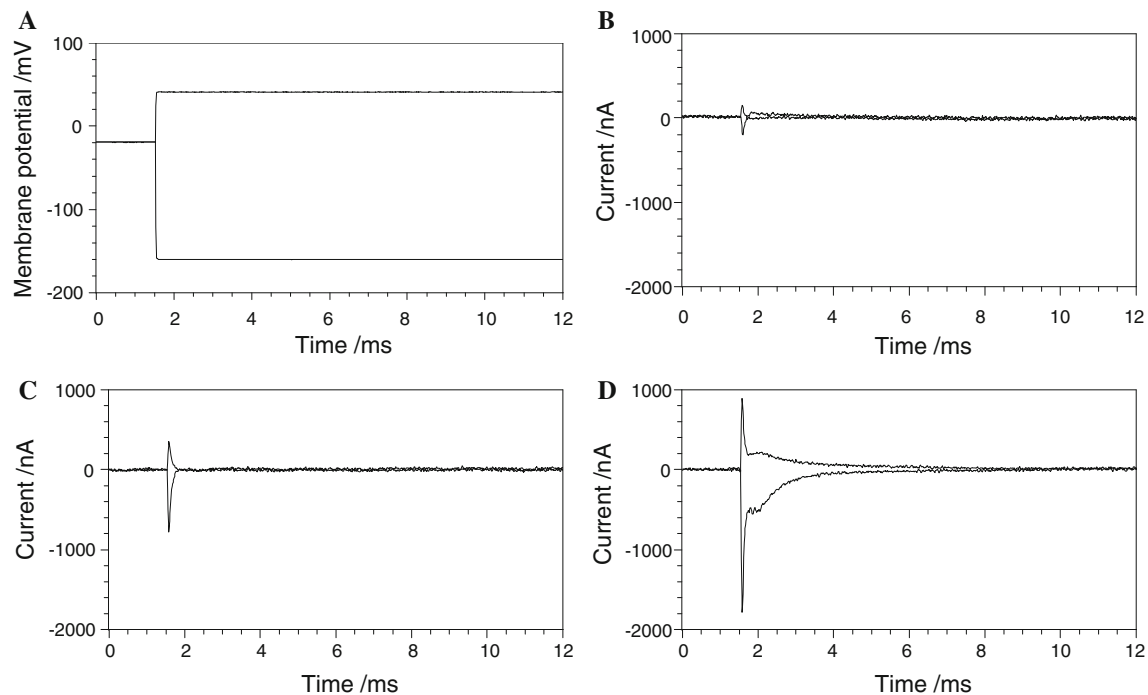


**Fig. 9** The inhibition by 3.2  $\mu\text{M}$  oligomycin B of transient currents mediated by mutant *Bufo* NKA: G813A. **a** Voltage steps used to elicit subtracted transient currents shown in **b–d**. **b** Control before the addition of oligomycin and ouabain. This subtracted current had a

similar duration compared to **c** and **d**. **c** Transient currents inhibited by 3.2  $\mu\text{M}$  oligomycin B. **d** Transient currents not inhibited by 3.2  $\mu\text{M}$  oligomycin B but by 1 mM ouabain

0.06 ms (Fig. 9c). The remaining fast component in the 3.2  $\mu\text{M}$  oligomycin B–uninhibited current (Fig. 9d) had a similar time constant ( $\tau = 0.05$  ms). As the concentration of oligomycin B was increased to 12.8  $\mu\text{M}$ , the fast component was almost completely inhibited (Fig. 10).

## Discussion

### The Partial Inhibiting Effect of Oligomycin on Transient Currents Mediated by Wild-Type *Bufo* NKA

The inhibition of  $I_p$  mediated by wild-type *Bufo* NKA was close to 100% at 120  $\mu\text{g}/\text{ml}$  oligomycin, but the transient currents were less sensitive to this concentration. The maximum inhibition of  $Q_{\text{all}}$  by oligomycin was about 70.8% (Fig. 2), which was consistent with previous findings (Holmgren and Rakowski 1994). A detailed analysis of transient currents before and after addition of oligomycin indicated that the faster charge movement was sensitive to oligomycin. Application of 120  $\mu\text{g}/\text{ml}$  oligomycin inhibited most of the faster component as indicated by the disappearance of the peak of the ouabain-sensitive transient currents after oligomycin application (Fig. 3).

### Oligomycin Preferably Inhibited Fast Charge Translocation Mediated by Wild-Type *Bufo* NKA and Increased Apparent $\text{Na}^+$ Binding Affinity

In the absence of oligomycin,  $Q_{\text{all}}$  is comprised of fast, medium and slow components. The fast component has a shallow slope (about 0.26) and the medium and slow components have steeper slopes (above 0.6) (Hilgemann 1994; Holmgren et al. 2000). In this study, we found that the slow component had a  $z$  value of 0.68 (Fig. 5). The  $Q_{\text{all}}$  vs.  $V$  curve had a  $z$  value of 0.4, which was intermediate between the  $z$  values of the fast (about 0.26) and slow (0.68) components (Fig. 4). Application of 120  $\mu\text{g}/\text{ml}$  oligomycin increased the  $z$  value of  $Q_{\text{all}}$  from 0.4 to 0.56, close to that of the slow charge movement ( $z = 0.68$ ). This also indicated that application of oligomycin diminished the component with a shallow slope, i.e., the fast component. Another effect of oligomycin on the  $Q_{\text{all}}$  vs.  $V$  curves was the rightward shift of  $V_{\text{mid}}$ , which indicated that the apparent binding affinity for  $\text{Na}^+$  was increased in the presence of oligomycin. The disappearance of charge movements with small dielectric coefficients and the increased apparent binding affinity for  $\text{Na}^+$  indirectly demonstrated that the presence of 120  $\mu\text{g}/\text{ml}$  oligomycin inhibited the fast charge translocation step ( $\text{E2P}\cdot\text{Na} \leftrightarrow \text{E2P} + \text{Na}_o$ ). Therefore, in the

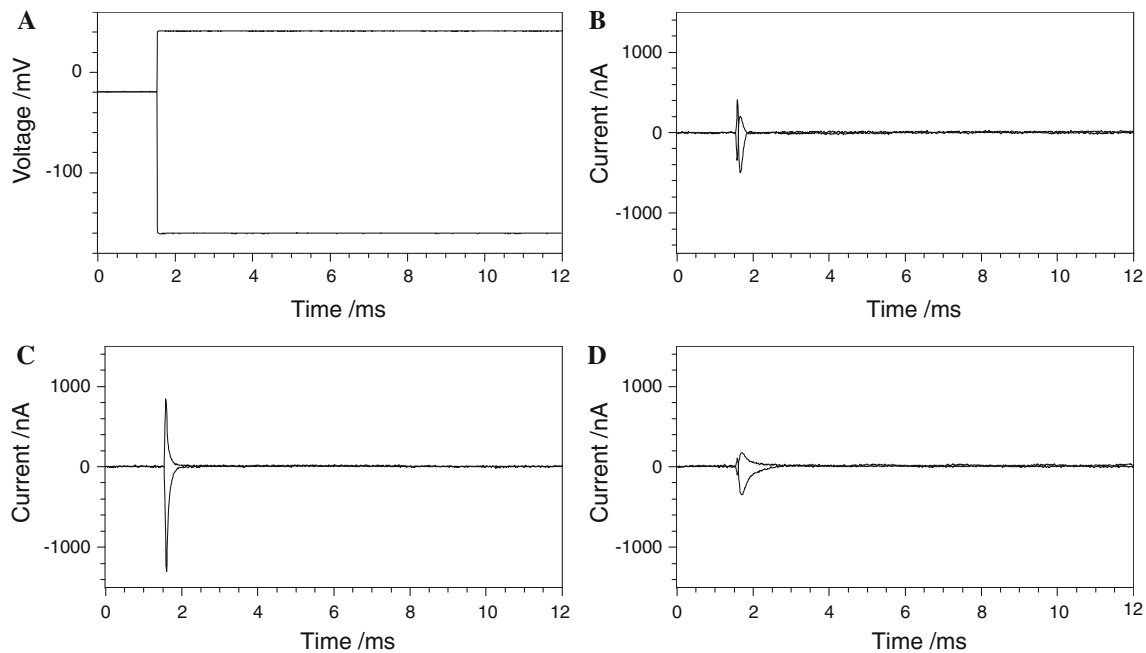


**Fig. 10** The inhibition by 12.8  $\mu\text{M}$  oligomycin B of transient currents mediated by mutated *Bufo* NKA: G813A. **a** Voltage steps used to determine the subtracted currents shown in **b–d**. **b** Control before the addition of oligomycin and ouabain. This subtracted

current had a similar duration to the currents in **c** and **d**. **c** Transient currents inhibited by 12.8  $\mu\text{M}$  oligomycin B. **d** Transient currents not inhibited by 12.8  $\mu\text{M}$  oligomycin B but by 1 mM ouabain

presence of oligomycin, most pumps could not go through this step to complete the full cycle and  $I_p$  was dramatically decreased.

The respective effects of oligomycin on these three components were demonstrated by studies on *Bufo* NKA: G813A due to the ability to utilize the P/4 voltage-clamp protocol in this preparation.

#### The Complete Sensitivity to Oligomycin of the Medium Component of Transient Currents Mediated by Mutant *Bufo* NKA: G813A

The transient current initiated by a voltage jump from  $-20$  to  $-160$  mV consisted of two components. The slower one ( $\tau$  is about 1–2 ms) was in the range of rate constants of the slow component determined from the subtracted ouabain-sensitive transient current. This portion of the transient current was not sensitive to oligomycin and was essentially unaltered after the application of oligomycin at saturating concentrations (Fig. 6c). Another transient component ( $\tau = 0.26$  ms) was similar to the medium component described by Holmgren et al. (2000) and sensitive to oligomycin (Fig. 6b). Therefore, after subtraction using the P/4 protocol, the medium and slow components were recorded; and of these, the medium component was sensitive to 120  $\mu\text{g}/\text{ml}$  of oligomycin at  $-160$  mV.

At  $V_h -20$  mV, some pumps were in the E1P(Na3) state, some in E2P·2Na and some in E2P. Note that because

the fast component caused by  $\text{Na}^+$  rebinding to E2P could not be observed with the P/4 protocol, E2P was considered to be the same as the E2P·1Na state. A voltage change from  $-20$  to  $-160$  mV caused  $\text{Na}^+$  to bind to empty binding sites of E2P·1Na and E2P·2Na, so we observed the medium and slow components, respectively. From previous studies, we know that oligomycin does not affect the conformational states and favors binding of  $\text{Na}^+$  (Glynn and Karlisch 1990; Arato-Oshima et al. 1996). We therefore speculate that oligomycin bound to E2P·2Na and blocked the reaction  $\text{E2P}\cdot 2\text{Na} \leftrightarrow \text{Na}^+ + \text{E2P}\cdot 1\text{Na}$ , which resulted in the elimination of the medium component in the presence of oligomycin (Fig. 6).

#### The Partial Sensitivity to Oligomycin of the Slow Component of Transient Currents Mediated by Mutant *Bufo* NKA: G813A

Due to the voltage dependence of charge translocation (Fig. 4), a voltage change from  $-20$  to  $20$  mV caused  $\text{Na}^+$  to be released from E1P(Na3) and E2P·2Na, and the slow and medium components, respectively, were observed in the transient current elicited by this voltage change (Fig. 6e, f). The medium component was completely sensitive to oligomycin, and the slow component of the transient current was partially sensitive to oligomycin. Figure 7 shows that the slow component was partially sensitive to oligomycin at positive membrane potentials but only

slightly inhibited by oligomycin at negative membrane potentials. The voltage-dependent response of the slow component to oligomycin can be explained by the sequential release of three sodium ions, which was previously demonstrated by Holmgren and colleagues (2000). In our study, the short-lived  $E2P \cdot 2Na$  was the form bound by oligomycin. Because the translocation of three sodium ions occurs sequentially,  $-20$  mV oligomycin reduced the number of pumps in  $E1P(Na_3)$  due to the increase in the number of pumps in  $E2P \cdot 2Na$  state due to oligomycin binding. Therefore, a smaller slow charge movement from  $E1P(Na_3)$  was measured when voltage steps to positive potentials were applied. This argument was supported by leftward-shifted  $Q_{slow}$  in the presence of oligomycin. The opposite effects of oligomycin to  $V_{mid}$  of  $Q_{slow}$ , as compared to  $V_{mid}$  of  $Q_{all}$  (Fig. 4), indicated that oligomycin affected the apparent binding affinity for  $3Na^+$  differently, that is, decreased the affinity to the first  $Na^+$  and increased the affinity for the other two  $Na^+$ .

Because the slow and medium components represent the first and second  $Na^+$  ions releasing from their binding sites, there are two possible explanations to the selective effects of oligomycin on the medium component. One is that the independence of the slow from the medium components resulted from the difference in releasing pathways of these two  $Na^+$  ions. When oligomycin “bound” to  $E2P \cdot 2Na$  in some way, the releasing pathway of the first  $Na^+$  (forming the slow component of transient current) was not affected by oligomycin but the releasing pathway for the second  $Na^+$  (forming the medium component of transient current) was blocked by oligomycin. Another possible explanation is that oligomycin inhibited the conformational change brought about by the release of the first  $Na^+$  and that this conformational change is required for the release of the other two  $Na^+$ . Our data do not provide evidence to distinguish between these two possibilities.

#### The Complete Sensitivity to Oligomycin of the Fast Component of Transient Currents Mediated by Mutant *Bufo* NKA: G813A

In the presence of a low concentration of oligomycin B, only a portion of the fast component with a time constant of  $0.05$  ms was inhibited (Fig. 9). As oligomycin B was increased to a more saturating concentration of  $12.8$   $\mu M$ , most of the fast component was inhibited (Fig. 10). The release of the third  $Na^+$  (forming the fast component of the transient current) was also blocked by oligomycin, which suggests that the release of the third  $Na^+$  might share the same mechanism with the second  $Na^+$  (Takeuchi et al. 2008). Oligomycin blocked the release of the second and third  $Na^+$  by either obstructing their specific ion pathway

or by preventing the conformational transition preceding the entry of these two ions into the single ion pathway.

#### Possible Future Applications of Oligomycin in Studying $Na^+/K^+$ -ATPase

The study of NKA treated with palytoxin has demonstrated that a single ion pathway traversed palytoxin-bound  $Na^+/K^+$  pump channels from one side of the membrane to the other (Takeuchi et al. 2008). However, the palytoxin-bound  $Na^+/K^+$  pump channel is not a native form of NKA. Further investigation of the accessibility of introduced cysteine residues in the ion pathway by water-soluble, sulfhydryl-specific reagents in the absence and presence of oligomycin may provide further insights as to whether this is the releasing pathway shared by three sodium ions. If there is only one pathway, the application of oligomycin will block the accessibility of residues located on the ion pathway. On the contrary, if oligomycin, a reagent inhibiting the release of two out of three sodium ions, cannot prevent water-soluble, sulfhydryl-specific reagents from accessing these residues, separate pathways probably exist.

#### Summary

The effects on transient currents strongly suggested that oligomycin blocks release/rebinding of two  $Na^+$  ions involved in the medium and the fast components of charge translocation in  $Na^+/Na^+$  exchange mode.  $E2P \cdot 2Na$  is proposed to be the state bound by oligomycin, and the reaction in the presence of oligomycin is proposed to be  $E1 + ATP + 3Na_i \leftrightarrow E1P(Na_3) \leftrightarrow E2P \cdot 2Na + Na_o$ . The slow charge movement from this population of pumps was not affected by oligomycin.

**Acknowledgments** Dr. Robert. F. Rakowski died unexpectedly during the later phase of this investigation (February 19, 2008), and we received substantial assistance from several individuals as we completed this work. We express our sincere thanks to Dr. M. Holmgren for instructive help on data collection; to Dr. R. A. DiCaprio for assistance with editing; to Dr. D. Gadsby for critical comments on the manuscript; to Dr. J. D. Horisberger and Dr. O. Capendeguy for providing cDNA of *Bufo* NKA  $\alpha_1$  and  $\beta_1$ ; and to reviewers for critical comments. This research was supported by NIH grant NS-022979 (to R. F. R.).

#### References

- Albers RW (1967) Biochemical aspects of active transport. *Annu Rev Biochem* 36:727–756
- Andersen OS, Silveira JEN, Steinmetz PR (1985) Intrinsic characteristics of the proton pump in the luminal membrane of a tight urinary epithelium. *J Gen Physiol* 86:215–234

- Arato-Oshima T, Matsui H, Wakizaka A, Homareda H (1996) Mechanism responsible for oligomycin-induced occlusion of  $\text{Na}^+$  within Na/K-ATPase. *J Biol Chem* 271:25604–25610
- Bezanilla F, Armstrong CM (1977) Inactivation of the sodium channel. I. Sodium current experiments. *J Gen Physiol* 70: 549–566
- De Weer P (1970) Effects of intracellular adenosine-5'-diphosphate and orthophosphate on the sensitivity of sodium efflux from squid axon to external sodium and potassium. *J Gen Physiol* 56:583–620
- Ding Y, Rakowski R (2010) The effect of holding potential on charge translocation by the  $\text{Na}^+/\text{K}^+$ -ATPase in the absence of potassium. *J Membr Biol* 236:203–214
- Esmann M, Skou JC (1985) Occlusion of  $\text{Na}^+$  by the Na,K-ATPase in the presence of oligomycin. *Biochem Biophys Res Commun* 127:857–863
- Fahn S, Koval GJ, Albers RW (1966) Sodium–potassium-activated adenosine triphosphatase of electrophorus electric organ. I. An associated sodium-activated transphosphorylation. *J Biol Chem* 241:1882–1889
- Gadsby DC (2007) Structural biology: ion pumps made crystal clear. *Nature* 450:957–959
- Gadsby DC, Kimura J, Noma A (1985) Voltage dependence of Na/K pump current in isolated heart cells. *Nature* 315:63–65
- Gadsby DC, Nakao M, Bahinski A (1989) Voltage dependence of transient and steady-state Na/K pump currents in myocytes. *Mol Cell Biochem* 89:141–146
- Gadsby DC, Rakowski RF, De Weer P (1993) Extracellular access to the Na,K pump: pathway similar to ion channel. *Science* 260:100–103
- Garrahan PJ, Glynn IM (1967) The stoichiometry of the sodium pump. *J Physiol* 192:217–235
- Glynn IM, Hoffman JF (1971) Nucleotide requirements for sodium-sodium exchange catalysed by the sodium pump in human red cells. *J Physiol* 218:239–256
- Glynn IM, Karlisch SJD (1990) Occluded cations in active transport. *Annu Rev Biochem* 59:171–205
- Hilgemann DW (1994) Channel-like function of the Na,K pump probed at microsecond resolution in giant membrane patches. *Science* 263:1429–1432
- Holmgren M, Rakowski RF (1994) Pre-steady-state transient currents mediated by the Na/K pump in internally perfused *Xenopus* oocytes. *Biophys J* 66:912–922
- Holmgren M, Wagg J, Bezanilla F, Rakowski RF, De Weer P, Gadsby DC (2000) Three distinct and sequential steps in the release of sodium ions by the  $\text{Na}^+/\text{K}^+$ -ATPase. *Nature* 403:898–901
- Jaisser F, Canessa CM, Horisberger JD, Rossier BC (1992) Primary sequence and functional expression of a novel ouabain-resistant Na,K-ATPase. The beta subunit modulates potassium activation of the Na,K-pump. *J Biol Chem* 267:16895–16903
- Kimura J, Miyamae S, Noma A (1987) Identification of sodium calcium exchange current in single ventricular cells of guinea-pig. *J Physiol* 384:199–222
- Läuger P (1991) *Electrogenic ion pumps*. Sinauer, Sunderland
- Li C, Capendeguy O, Geering K, Horisberger J-D (2005) A third  $\text{Na}^+$ -binding site in the sodium pump. *Proc Natl Acad Sci USA* 102:12706–12711
- Morth JP, Pedersen BP, Toustrup-Jensen MS, Sorensen TLM, Petersen J, Andersen JP, Vilsen B, Nissen P (2007) Crystal structure of the sodium–potassium pump. *Nature* 450:1043–1049
- Nakao M, Gadsby DC (1986) Voltage dependence of Na translocation by the Na/K pump. *Nature* 323:628–630
- Post RL, Hegyvary C, Kume S (1972) Activation by adenosine triphosphate in the phosphorylation kinetics of sodium and potassium ion transport adenosine triphosphatase. *J Biol Chem* 247:6530–6540
- Rakowski RF, Paxson CL (1988) Voltage dependence of Na/K pump current in *Xenopus* oocytes. *J Membr Biol* 106:173–182
- Rakowski RF, Gadsby DC, De Weer P (1989) Stoichiometry and voltage dependence of the sodium pump in voltage-clamped, internally dialyzed squid giant axon. *J Gen Physiol* 93:903–941
- Sagar A, Rakowski RF (1994) Access channel model for the voltage dependence of the forward-running  $\text{Na}^+/\text{K}^+$  pump. *J Gen Physiol* 103:869–893
- Skou JC, Esmann M (1992) The Na,K-ATPase. *J Bioenerg Biomembr* 24:249
- Takeuchi A, Reyes N, Artigas P, Gadsby DC (2008) The ion pathway through the opened  $\text{Na}^+/\text{K}^+$ -ATPase pump. *Nature* 456:413–416
- Yang XC, Sachs F (1989) Block of stretch-activated ion channels in *Xenopus* oocytes by gadolinium and calcium ions. *Science* 243:1068–1071
- Yoda S, Yoda A (1986) ADP- and  $\text{K}^+$ -sensitive phosphorylated intermediate of Na,K-ATPase. *J Biol Chem* 261:1147–1152